Quantum Chemical Investigations on C14C10-Branched-Chain Glucoside Isomers Towards Understanding Self-Assembly

Bayach, Imene*[+]

Department of Chemistry, College of Science, King Faisal University, Al-Hofuf, 31982 Al-Ahsa, SAUDI ARABIA

Tan, Teng Yong; Manickam Achari, Vijay; Hashim, Rauzah

Center for Fundamental and Frontier Sciences in Nanostructure Self-Assembly, Department of Chemistry, Faculty of Science, University of Malaya, 50603 Kuala Lumpur, MALAYSIA

ABSTRACT: *Density Functional Theory (DFT) calculations have been carried out using a Polarizable Continuum Model (PCM) in an attempt to investigate the electro-molecular properties of branched-chain glucoside ($C_{14}C_{10}$-D-glucoside) isomers. The results showed that α-configuration of pyranoside form is thermodynamically the most stable, while the solution should contain much more β than α, according to the calculated Boltzmann distribution. Additionally, $C_{14}C_{10}$-β-D-xylopyranoside is studied for comparison with its glucoside analogue in order to investigate the electronic effect of the hydroxymethyl ($-CH_2$-OH) group at position 5-C. The topological parameters of intramolecular X-H···Y hydrogen bonds were analysed and the nature of these interactions were considered using the Atoms in Molecules (AIM) approach. Moreover, natural bond orbital analysis (NBO) was performed to define bond orders, charge and lone pair electrons on each atom and effective non-bonding interactions. HOMO/LUMO analysis allowed the description of investigated isomers and led to a further understanding of their behaviours. The computational results, especially intramolecular hydrogen bonding and molecular electronic potential analysis are directly relevant to liquid crystal self-assembly and membrane biophysics.*

KEYWORDS: *Guerbet Glycolipids; $C_{14}C_{10}$-D-glucoside; hydrogen bonding; DFT; AIM; NBO.*

INTRODUCTION

The difficulties encountered on studying liquid crystal models due to their complexities make a computational approach increasingly relevant. Liquid crystal science is challenging and attractive field due to its wide range of applications including organic, electronics, optics and nanostructured materials. Liquid crystal is defined as a distinct state of matter that exhibits features from both solid and fluid states. Accordingly, it has ordering properties of solids but flows like liquids.[1] Constituent molecules in liquid crystalline state display variety

* *To whom correspondence should be addressed.*
+ E-mail: ibayach@kfu.edu.sa
1021-9986/20/3/ 257-269 13/$/6.03

of structurally self-assembled ordered phases, each with distinct physical properties, which make them attractive for diverse applications.[2]–[6] Amphiphilic glycolipids exhibit both thermotropic and lyotropic liquid crystalline properties [7] giving rise to ordered phases such as lamellar, hexagonal and cubic phases, which may have diverse technical and biological applications in e.g., lubricants, drug delivery as well as solubilization and crystallization of membrane enzymes [2, 4, 8].

Compared to the common liquid crystal surfactants, either those prepared from natural resources that are frequently difficult to extract with high purity or those consisting of synthetic inorganic materials that although "cheap" are usually not environmentally friendly, surfactants from glycolipids provide an excellent alternative. Additionally, their low toxicity, biodegradability, and non-immunogenicity, allow active materials to be encapsulated and discharged at a sustained rate to reduce the side effects of the rapid burst drug release.[4]

Understanding the effect of structural features on the thermotropic and lyotropic assemblies is a key step toward rational design of new glycolipid-based materials. The liquid crystallinity in glycolipids is influenced by different parameters including the type of alkyl chain used as hydrophobic part and the sugar headgroup as hydrophilic part.[9] Our previous investigations into structure-property relationships from computational studies provide an important molecular basis for future designing new synthetic glycolipid materials. [9]–[12] Nevertheless, many properties of glycolipids are not fully understood, which calls for a rigorous systematic structure-property relationship study. Previously, the properties of different straight chain glycolipids have been studied using DFT calculation. For example, Mosapour Kotena et al. used B3LYP/6-31G level of theory for conformational analysis of n-octyl-α/β-*D*-mannopyranoside as well as two other glycosides, namely, n-octyl-β-*D*-glucopyranoside and n-octyl-β-*D*-galactopyranoside. The effect of the hydroxyl group's orientations (axial vs. equatorial) either at the C1 or C4 position has been evaluated. It has been shown that the number of intramolecular hydrogen bond is directly correlated with the corresponding stability of the investigated glycolipids and probably involved at their stability in the self-assembly phenomena.[13, 14] Moreover, DFT calculations at the B3LYP/6–31 + G(d,p) level of theory has been applied on the investigation of octyl-*D*-xyloside isomers in order to explain the features responsible for the liquid crystal mesophases. Compared to a glucoside, a xyloside has a reduced headgroup volume that makes it less hydrophilic. Here again, the role of intramolecular hydrogen bonding was highlighted for participating to control the relative stability of each isomer. Our results have provided new features that are probably responsible for forming two non-equivalent inverse micelles, which are self-assembled into a cubic discontinuous phase with a space group of *Fd3m* commonly found for xylosides. Also our calculations for these xylolipids helped at demonstrating sugar amphoterism, which is implicated in the heterogeneity nature of lipid self- assembly.[12]

In the present work, we are using similar strategy to investigate one branched chain glycolipid, namely ($C_{14}C_{10}$)-branched-chain glucoside by considering its isomers.

Interestingly, *Liew et al.* [9] reported the thermotropic and lyotropic phases of highly pure synthetic Guerbet glycolipids, using differential scanning calorimetry, optical polarizing microscopy and small-angle X-ray scattering. This glycolipid family is prepared using a glycosidation procedure that involves reacting a protected sugar with Guerbet alcohol. Guerbet alcohols have been introduced for over 100 years since *Marcel Guerbet* initiated the basic chemistry in the 1890s. [15] This chemistry, which bears his name, has made possible the synthesis of a regio-specific, beta-branched hydrophobe, which introduces high-purity branching into the molecule. Guerbet alcohols contain two asymmetric chains that differ by two methylene units, and branch at the β-carbon position, which is chiral.[15] Indeed, the double alkyl chains glycolipids were reported to promote inverse phases.[11, 16, 17] More specifically, the branched-chain glycolipids are more likely to adopt non-lamellar phases such as bicontinuous cubic phase, inverse hexagonal phase and inverse micellar cubic phase, compared to their mono-alkylated counterparts.[18] For instance, branched glucolipids exhibit inverted hexagonal phase that is important for many biological processes in nature. In addition, the Guerbet glycosides favor the stable formation of a bicontinuous cubic phase with the space group of *Ia3d* in excess water.[11] This feature is rare amongst other lipidic phases and is probably due to the presence of chain asymmetry in the Guerbet glycoside.[11]

The amphiphilic nature of these compounds coupled with their ability to form inverse non-lamellar phases at room temperature makes them ideal candidates

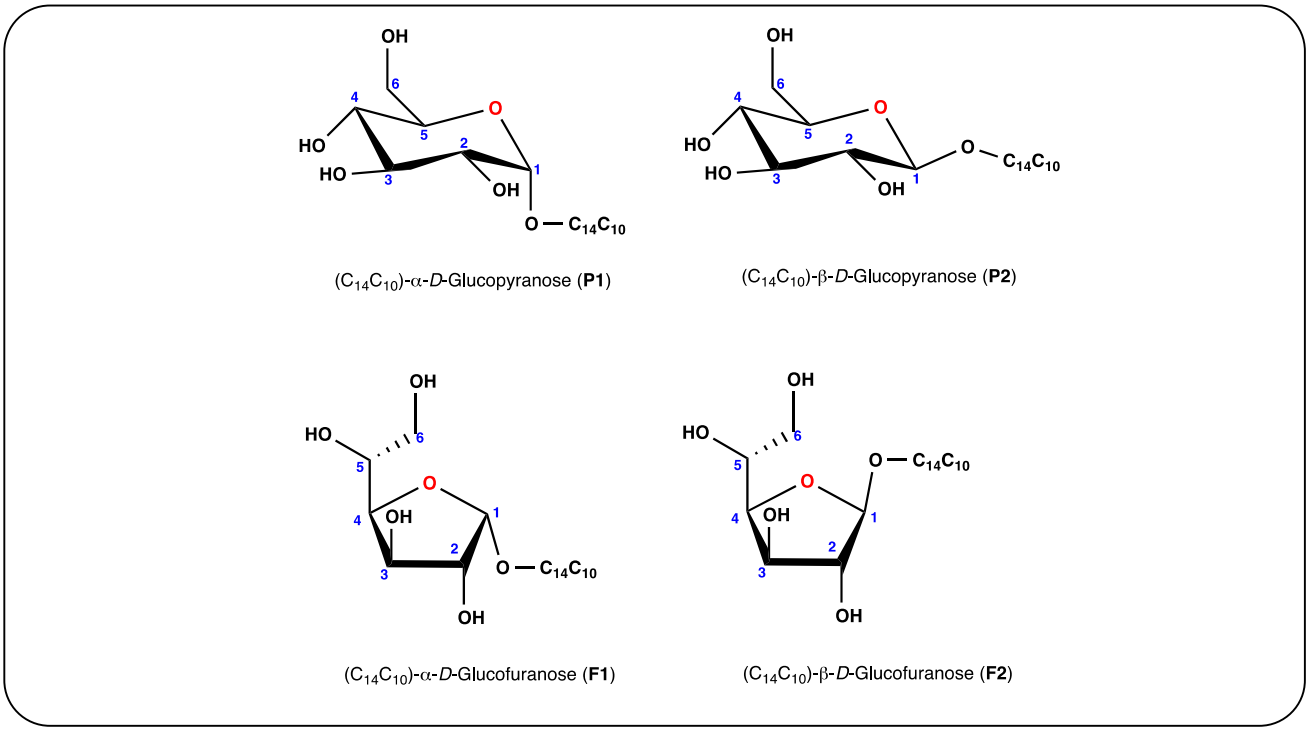

Fig. 1: Chemical structures of the branched chain ($C_{14}C_{10}$)-D-glucoside isomers. The number indicates carbon atom position.

for promising uses [9]. Additionally, the branched-chain glycolipids are isostearic to many natural lipids and thus have the propensity to mimic the property and function of natural lipids. Thus, due to their interesting and diverse applications, the present work is dedicated to study ($C_{14}C_{10}$)-branched-chain glucoside isomers (Fig. 1) in order to rationalize their molecular features toward understanding the structure/property relationship, using computational tools. The $C_{14}C_{10}$-β-*D*-xylopyranoside was also studied for comparison purpose.

Computational methods

Geometry optimization of $C_{14}C_{10}$-branched-chain glucoside isomers were carried out using Density Functional Theory (DFT) with the hybrid B3LYP exchange-correlation functional [19], [20] coupled with 6-31+G(d,p) basis set for all the atoms. In order to confirm the stable minima in potential energy surface, frequency calculations were carried out at the same level of theory, i.e., B3LYP/6-31+G(d,p). The absence of imaginary frequencies confirms the ground states minima. Atoms In Molecules (AIM) theory [21] and Natural Bond Orbital (NBO) analysis [22] were used to analyse hydrogen bonding. The Molecular Orbital (MO) analysis was investigated using the Time Dependent Density Functional Theory (TD-DFT) formalism [23] at the same level of theory. Molecular Electrostatic Potentials (MEPs) have been applied to elucidate electronic properties of the investigated molecules. The solvent effects were taken into account implicitly, using the Polarizable Continuum Model (PCM) in which the solute is embedded into a shape-adapted cavity surrounded by a structure-less continuum that is described as a dielectric continuum characterized by its dielectric constant. The use of PCM correctly allows modelling the major solvent effects.[24] Water was selected as being the solvent used to measure the physico-chemical properties of molecules. All calculations have been performed using Gaussian 09.[25] Both GaussView [26] and VMD (Visual Molecular Dynamics) [27] software were used for visualizing molecules.

RESULTS AND DISCUSSION

Energy calculations

Fig. 1 illustrates basic chemical structures of the investigated systems, i.e., $C_{14}C_{10}$-*D*-glucoside isomers, including pyranoside and furanoside as well as anomeric forms (α and β), although Fig. 2 represents the optimized geometries of the same isomers. The energetic values

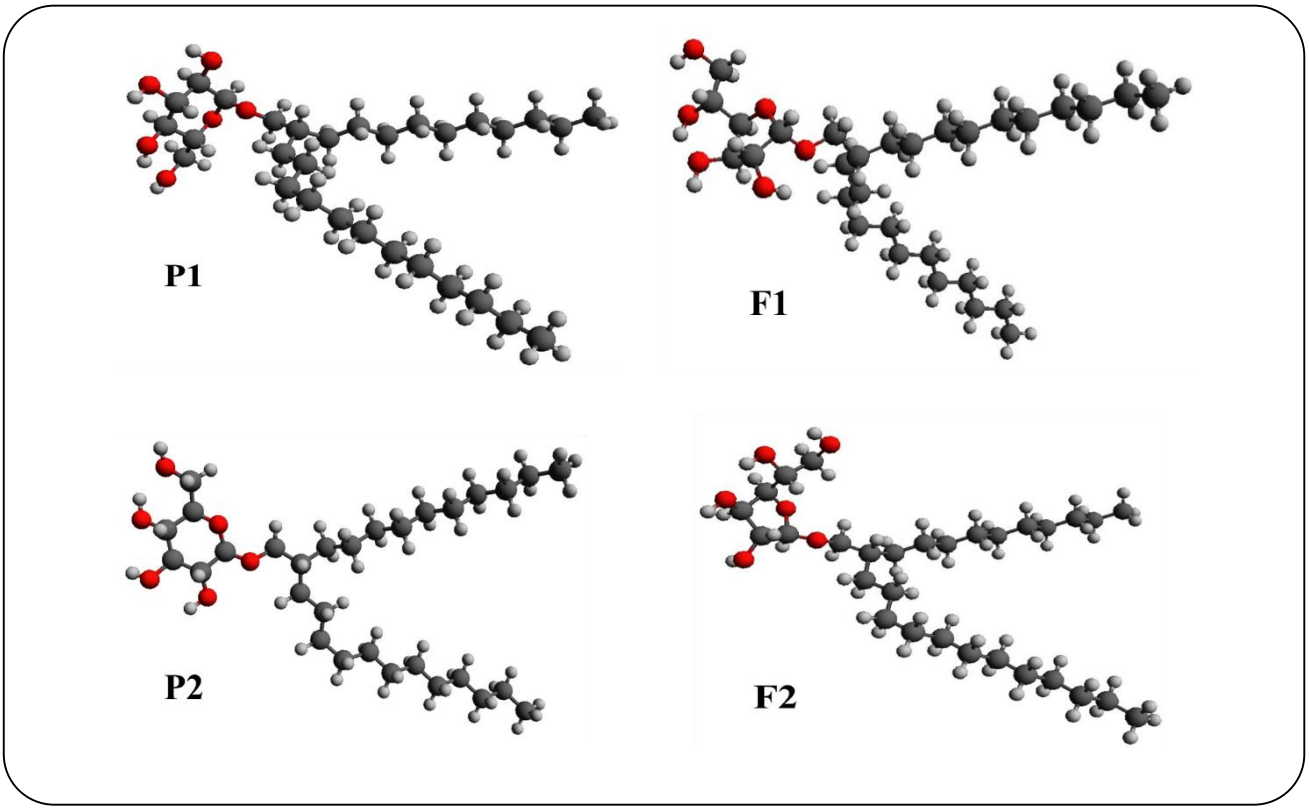

Fig. 2: B3LYP/6-31+G(d,p)-Optimized structures.

obtained in PCM of the most stable conformations are shown in Table 1. The six-membered pyranose ring includes a C5O ring (**P1** for α and **P2** for β), while the five-membered furanose ring forms a C4O ring (**F1** for α and **F2** for β). Since we already demonstrated that the solvent stabilizes alkyl glycolipids [12]–[14] and we are particularly interested on studying the behaviors of these molecules in water, only quantum mechanics-based calculations in solvent phase were considered. The free Gibbs energies for the investigated glucosides reveal that the $C_{14}C_{10}$-α-*D*-glucofuranoside (**F1**) is thermodynamically the most stable followed by $C_{14}C_{10}$-β-*D*-glucopyranoside (**P2**), with only 0.55 kcal/mol of relative Gibbs free energy difference, then $C_{14}C_{10}$-α-*D*-glucopyranoside (**P1**), and $C_{14}C_{10}$-β-*D*-glucofuranoside (**F2**) (Table 1). The relative Gibbs free energy of **P2** with regard to the stable **P1** is 0.67 kcal/mol (Table 1), which is close to that reported for to the *D*-glucopyranose enantiomers (0.35 kcal.mol^{-1}).[28] The Boltzmann distribution (D_{boltz}) is also calculated for all different isomeric forms (Table 1). The results showed that D_{boltz} of α (**P1**) and β (**P2**) pyranoside are 34.48 % and 23.96 %, respectively while that of α (**F1**) and β (**F2**) furanoside are 41.53 % 0.03 %, respectively. These results on branched-chain glucosides are consistent with previous experimental observations on glucopyranosides reporting a higher thermodynamic stability of the α pyranose compared to the β form in solution.[29] The small value of D_{boltz} for **F2** is coherent with that stated for their monosaccharides analogues.[28] In fact, β furanosides should occur in very small amount according to our current calculations of both D_{boltz} and ΔG_{rel} (Table 1), which is similar to spectroscopic results from literature with respect to their monosaccharide analogues indicating that too little of furanose forms has detected for glucose.[28] Comparison of furanoside anomers reveals that the α (**F1**) is more favorable compared to the β (**F2**), with a free-energy difference of 3.60 kcal/mol (Table 1).

The structures of investigated cyclic forms are greatly stable due to the high stability of the intramolecular hemiacetal involving five or six atoms for furanose and pyranose, respectively. Hence, it is thermodynamically unfavorable to form the acyclic forms. For instance, equilibrium solution of *D*-glucose contains only 0.0026 %,

Table 1: Calculated Free Gibbs energies G (kcal/mol), corresponding relative Gibbs ΔG_{rel} (kcal/mol), Boltzmann distribution D_{boltz} (%) and dipole moment μ (Debye) of the investigated molecules in solvent phase.

	G	ΔG_{rel}	D_{boltz}	μ
P1	-1022876.90	1.23	34.48	5.02
P2	-1022877.58	0.55	23.96	5.18
F1	-1022878.13	0.00	41.53	5.66
F2	-1022874.53	3.60	0.03	6.06

of the acyclic form, as determined by polarography.[30] That explains the reason for studying only the cyclic isomers in the present work.

We noticed that intramolecular hydrogen bonding significantly contributes to stabilize the investigated molecules. Further analyses will be given in the next section that is dedicated to hydrogen bond analysis.

We calculated the dipole moment (μ) that indicates the net molecular polarity for each isomer. The order of dipole moment values for the different isomers from the higher to the lowest μ is as follow: μ(**F2**)> μ(**F1**)>μ(**P2**)> μ(**P1**), indicating that **F2** is the most polar (i.e., most electronegative) (Table 1). Consequently, the β anomer is more polar than the α for both furanosides and pyranosides. As previously observed for octyl xylosides,[13] the furanosides have higher dipole moment than pyranosides. This difference on dipole moment, which is related to electrophilicity, affects the behaviors of these glycolipids in self-assembly and influences their liquid crystalline properties. This difference in dipole moment between isomers induces a difference in electronegativity, which could explain the formation of hexagonal H_{II} phases in self-assembly structure which often found in the long chain Guerbet compounds such as the molecules ($C_{10}C_{14}$) under investigation.[18] It is possible that this difference together with the asymmetric nature of the branched chain might contribute to stabilize the inverse bicontinuous cubic phase of space group Ia3d in excess water, but the mechanism of this formation is not clear at present. It will be interesting to control such an excess water Ia3d phase due to its interesting applications in e.g., templating, encapsulation and membrane protein crystallization.

Atoms In Molecules analysis

The topological analysis of the electron density using the AIM methodology [31] shows the presence of different bond critical points (BCP) between O and H (Fig. 3 and Table 2). The molecular graphs confirmed the presence of one hydrogen bond (HB) for **P1**, **P2** and **F2**, while two hydrogen bonds were observed for **F1**. Different parameters such as the Laplacian of the charge density ($\nabla^2\rho(r)$), the total electron energy density ($H(r)$) at the BCP and the ellipticity (ε) are used to describe hydrogen bonding.[31]–[33] The positive sign of the $\nabla^2\rho(r)$ for all the above hydrogen bonding indicates local charge depletion. Additionally, the negative sign of $H(r)$ implies that the corresponding hydrogen bonds are classified as relatively strong and partially covalent-partially electrostatic (Pc–Pe).[34] Hence, all the investigated hydrogen bonds are classified as (Pc–Pe) excluding the $O_2H\cdots O_1$ (**F1**) for which the local total electronic energy is $+14.36\times10^{-4}$ kcal/mol and thus indicative of a slightly less stabilizing interaction. Moreover, by considering the ε values, we conclude that the intramolecular HB $O_2H\cdots O_1$(**F1**) is the least stable compared to all other hydrogen bonds. This agrees with its corresponding length (2.15 Å) that confirms it as the weakest hydrogen bonding.

The stability of intramolecular hydrogen bonding can be further described by the molecular graph since it shows the pseudo-rings formed by the investigated H-bond (Fig. 3). Indeed, for all stable hydrogen bonds (i.e., all the investigated except $O_2H\cdots O_1$), the H atom of the O_xH_x establishes an H-bond with the O atom of the O_yH_y, thus forming a 6-membered pseudo-ring. Conversely, $O_2H\cdots O_1$ forms 5-membered pseudo-ring, which is, by definition, more strained and does not allows strong H-bonds. Consequently, from the present AIM results of branched glucosides, the intramolecular hydrogen bonds are stable for both pyranosides and furanosides and confirm our assumption of the stabilizing role of the hydroxymethyl (−CH_2-OH) group.

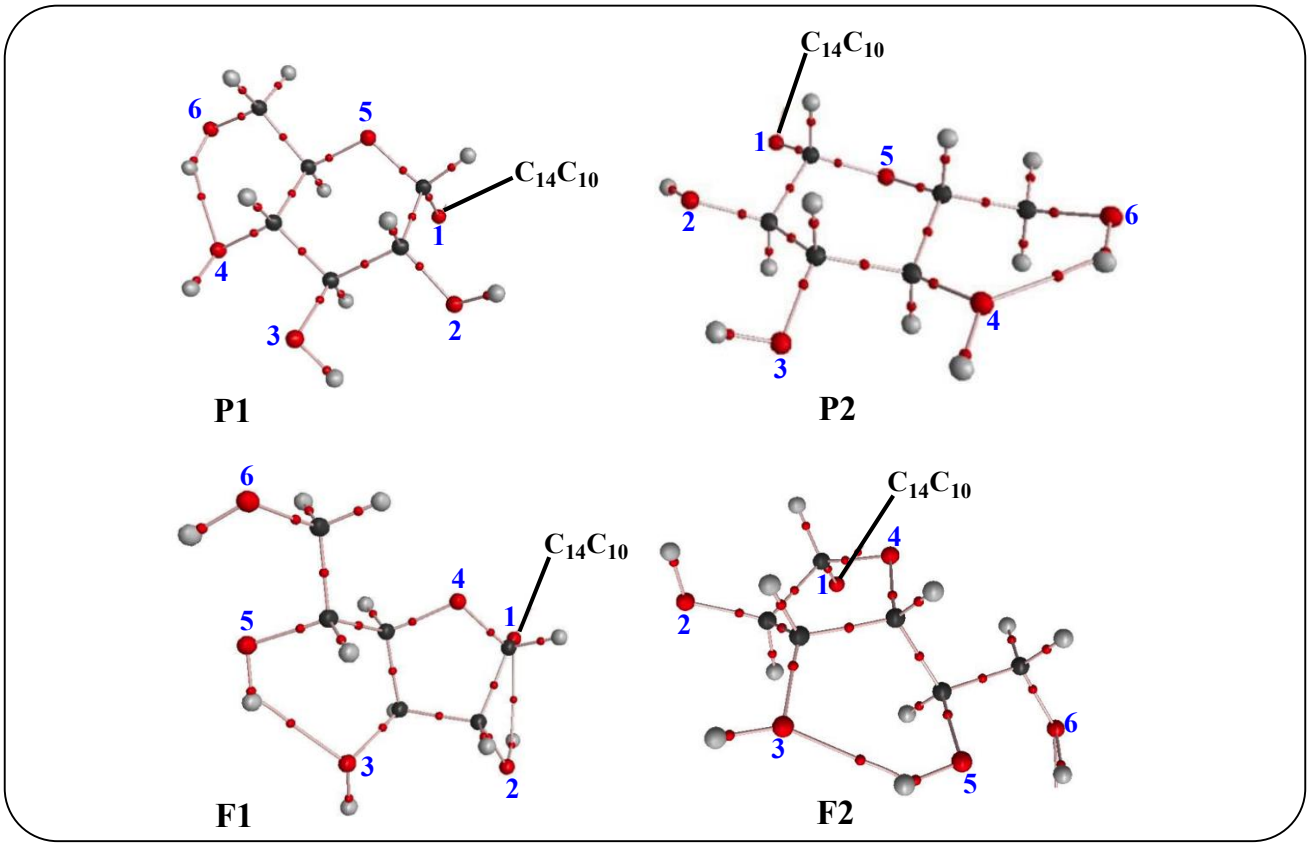

Fig. 3: Molecular graph of intramolecular hydrogen bonding. Numbers indicate the oxygen position

The current AIM analysis allows investigating only hydrogen bonds that have lengths lower than 2.3 Å. This software limitation prevents the investigation of HB with higher length such as $O_6H\cdots O_5$ (2.31 Å) that we noticed in both furanoside anomers (**F1** and **F2**). This means that furanosides have more intramolecular hydrogen bonding than pyranosides.

It is also interesting to note that for **P1** and **P2**, there are two OH groups on 2-C and 3-C, which do not involve in intramolecular hydrogen bond. This is easily visible from the calculated AIM molecular graph (Fig. 3). Therefore, we can assume that in a self-assembly these two hydroxyl groups can participate in bonding with another lipid within the layer (intralayer bonding) or with another lipid from the next layer (interlayer) or solvent (if present) such as water (Fig. 4). If water is present, it can be clearly seen that the 3-OH is more likely to be bonded to water than the 2-OH since the former resides farther from the chain/headgroup interface. As one hydroxyl group can be bonded to 1.8 water,[35], [36] this supports the previous observation we have made on the number of bound water for octyl-glucoside determined using deuterium NMR technique which was found to be about 1.7.[37] More interestingly, this assumption can be applied for furanosides, which are less abundant in solution than pyranosides and thereby making experiments on these five-membered ring glucolipids more challenging. Hence, in the case of the studied furanosides, the hydroxyl at 6-C will be more likely bonded to water. However, since **F1** lacks another hydroxyl group, it will probably not form a stable layer structure unlike **F2** that has two free hydroxyl groups. These expectations from the current investigations on the intramolecular HB could be verified by a subsequent Molecular Dynamic (DM) study.[38]

NBO analysis

The NBO analysis was applied to investigate the electronic interaction effect on the reactivity and behaviors of isomers that possess hydrogen bonds (Table 3). The formation of hydrogen bonding suggests the delocalization of certain electronic charge amount from the lone pair to the anti-bonding orbital. Herein, the electronic wave

Table 2: Topological parameters in solvent phase; the H-bond length (Å), the electron density at BCP ($\rho(r)$), its Laplacian ($\nabla^2\rho(r)$), the ellipticity (ε), the potential electron energy density ($V(r)$), the kinetic electron energy density ($G(r)$) and the total electron energy density at BCP ($H(r)$), in kcal/mol.

	H-bond (Å)	ρ(r) ($\times 10^{-2}$)	$\nabla^2\rho$(r) ($\times 10^{-2}$)	Ellipticity ε ($\times 10^{-2}$)	V(r) ($\times 10^{-2}$)	G(r) ($\times 10^{-2}$)	H(r) ($\times 10^{-4}$)
P1	$O_6H\cdots O_4$: 2.01	2.29	7.14	3.64	-1.88	1.83	-4.47
P2	$O_6H\cdots O_4$: 2.01	2.29	7.22	4.07	-1.89	1.85	-4.03
F1	$O_5H\cdots O_3$: 1.98 $O_2H\cdots O_1$: 2.15	2.54 1.81	8.14 7.49	2.10 105.72	-2.12 -1.59	2.08 1.73	-4.32 14.36
F2	$O_5H\cdots O_3$: 1.97	2.40	8.10	4.11	-2.02	2.02	0.29

Table 3: Second-order perturbation energies $E^{(2)}$ (donor →acceptor) at the B3LYP/6-31+G(d,p) level in solvent phase.

	Donor NBO(i) n(O)	Acceptor NBO(j) σ*(O-H)	$E^{(2)}$ kcal/mol[1]
P1	LP(2) O_6	BD*(1) $O_6H\cdots O_4$	5.65
P2	LP(2) O_6	BD*(1) $O_6H\cdots O_4$	5.48
F1	LP(2) O_5 LP(2) O_2	BD*(1) $O_5H\cdots O_3$ BD*(1) $O_2H\cdots O_1$	6.57 0.94
F2	LP(2) O_5	BD*(1) $O_5H\cdots O_3$	6.13

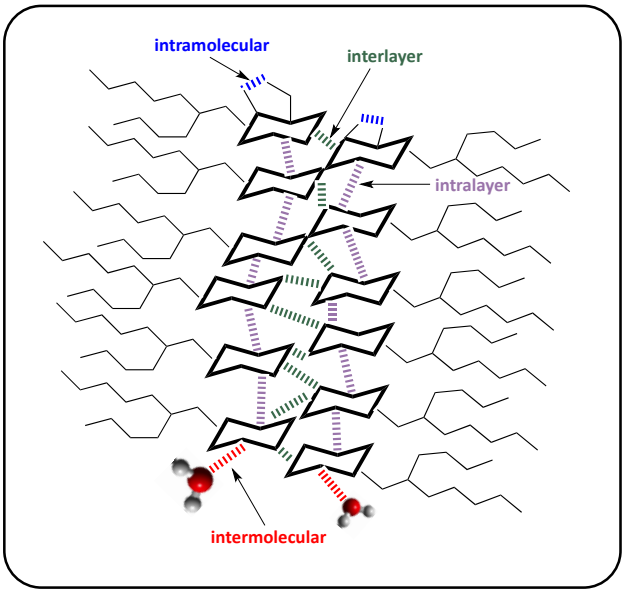

Fig 4: Schematic representation of different types of hydrogen bonding within glycolipid self-assembly

functions are interpreted in terms of occupied Lewis and unoccupied non-Lewis localized orbitals.[22] Hence, delocalization effects can be identified from the presence of off-diagonal elements of the Fock matrix. Moreover, the electronic charge is transferred from the *n*(O) lone electron pair orbital atom in donor fragment to the σ*(O-H) anti-bonding orbital of the acceptor fragment. This delocalization interaction is estimated from the second order perturbation energy ($E^{(2)}$) theory involving $i \rightarrow j$ delocalization as:

$$E^{(2)} = \Delta E_{ij} = q_i \frac{F(i,j)^2}{\varepsilon_j - \varepsilon_i},$$

where q_i is the donor orbital occupancy, ε_i and ε_j are orbital energies and $F(i,j)$ is the off-diagonal element.

In all cases, it can be seen that the σ*(O-H) antibonding participates as an acceptor and the oxygen lone pair as a donor in a charge transfer interaction. According to the NBO results that involve σ*(O-H) antibonding for the investigated molecules, the values of the stabilization energies $E^{(2)}$ in the $O_6H\cdots O_4$ are 5.65, 5.48 for **P1** and **P2**, respectively. These similar values indicate that these hydrogen bonds are of similar strength, which is in agreement with their corresponding lengths (Table 2). In the same way, $E^{(2)}$ in $O_5H\cdots O_3$ are 6.57 and 6.13 kcal/mol for **F1** and **F2**, respectively. Likewise, the lowest $E^{(2)}$ found for $O_2H\cdots O_1$ in **F1** would suggest that it is the most unstable hydrogen bonding (Table 3). Hence, according to data reported in Table 2 and Table 3, all the investigated hydrogen bonds are considerably stable except the weak $O_2H\cdots O_1$ in **F1**.

The presence of $-CH_2$-OH, (and ˜CH(OH)-CH_2-OH) groups in the glucosides implies the formation of stable hydrogen bonds in both pyranosides (and furanosides). In contrast, the absence of such group, as previously reported for the xylopyranosides [12]

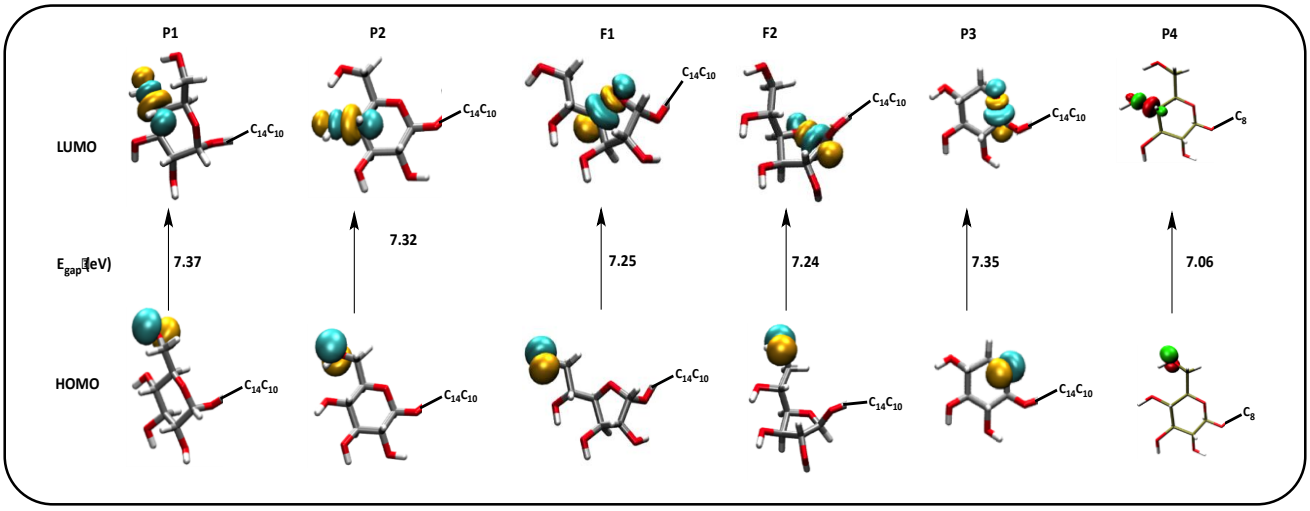

Fig. 5: Spatial distribution of MOs for the $C_{14}C_{10}$-D-glucoside isomers (P1, P2, F1 and F2), the $C_{14}C_{10}$-β-D-xylopyranoside (P3), and the C_8-β-D-xylopyranoside (P4) in PCM.

induces significantly weaker intramolecular hydrogen bond strengths. When the hydroxymethyl group is re-introduced into the structure of xylosides (xylofuranoside), the intramolecular hydrogen bonds become considerably stronger.

Electronic properties

Molecular orbital (MO) analysis

The MO analysis consists on the study of the two main orbitals involved in chemical stability and reactivity that are the highest occupied molecular orbital (HOMO) and the lowest unoccupied molecular orbital (LUMO). The HOMO spatial distribution is an indication of electron transfer zones. It is probably assisting the subsequent deprotonating site because the electrons involved in the electron transfer are those of the highest energy level. The more the HOMO level is delocalized, the more numerous are the electron transfer sites and more redox reactions will occur. [39] As it can be seen from Fig. 5, for both pyranosides and furanosides, the HOMO is located in the oxygen atom number six (6-O) of the hydroxymethyl group. This is different from the LUMO of the octyl single chain (P4) that we also investigate in this work and for which the LUMO is associated with 4-C (Fig. 5). However, the hydrogen bond lengths $O_6H\cdots O_4$ in these two systems (C_8- and $C_{14}C_{10}$-α/β-*D*-glucopyranoside) are similar (2.01 Å). We assume therefore that the chain branching does not significantly affect the intramolecular hydrogen bonding strength for the glucopyranosides, but will probably influence intermolecular (including intra- and interlayer) hydrogen bonding. Furthermore, some experiments showed that Guerbet glycosides have lower transition temperatures than single-chain glycosides, resulting from the chain branching that leads to an increase in conformational disorder in the hydrocarbon chain region due to an increase in chain hydrophobicity [11]. In the case of furanosides, the LUMOs for the α and β anomers (F1 and F2) are in 4-C and 1-C, respectively.

In general, the electronic transition from the HOMO to LUMO represents the energy gap (E_{gap}) that describes the molecular reactivity. The value of E_{gap} is directly correlated to the measure of the excitability of molecules; the smaller energy gap in a molecule, the easier its excitement, and vice versa. Moreover, the lower E_{gap} value would exhibit the eventual charge transfer interaction, which is generally responsible for the molecular bioactivity. Conversely, larger E_{gap} provides lower chemical reactivity because it is quite energetically unfavourable to add electrons to a high LUMO and to remove electrons from a low HOMO.[40] In solid-state physics, the band gap is a major factor determining the electrical conductivity of a solid. Large band gaps are generally affiliated to insulators, while substances with smaller band gaps are semiconductors and conductors are characterised by either a very small band gaps or none, because

Table 4: (B3LYP/6-31+G(d,p))-Calculated energies of the frontier MOs ε_{HOMO}, ε_{LUMO} (eV); energy gap E_{gap} (eV); ionization potential IP (eV); electron affinity A (eV); hardness η (eV); chemical potential μ_P (eV); electrophilicity: ω (eV); softness S (eV^{-1}).

	P1	P2	F1	F2	P4
ε_{HOMO}	-7.53	-7.47	-7.37	-7.41	-7.31
ε_{LUMO}	-0.17	-0.15	-0.12	-0.18	-0.25
E_{gap}	7.37	7.32	7.25	7.24	7.06
IP	7.53	7.47	7.37	7.41	7.31
A	0.17	0.15	0.12	0.18	0.25
η	3.68	3.66	3.63	3.62	3.53
μ_P	-3.85	-3.81	-3.75	-3.80	-3.78
ω	4.02	3.97	3.87	3.98	4.05
S	0.27	0.27	0.28	0.28	0.28

the valence and conduction bands overlap. The E_{gap} values can be also correlated to the hardness/softness of molecules (i.e., hard molecules have a large E_{gap} and vice versa).[41] Thus, from the electro-molecular properties displayed in Table 4, we showed that furanosides are slightly softer than pyranosides, which is consistent with both their softness and hardness values as shown in Table 4. Moreover, we assume that branching of chain makes molecules harder according the E_{gap} values of **P2** (which present branched chain) and **P4** (which has a straight chain). The hardness (η) and softness (*S*) are important parameters to estimate for example the resistance to deform the electron cloud of the chemical system and the stability of chemical species. We also found that the calculated E_{gap} of these glucolipids are about 7 eV, which are interestingly similar to many other systems as that for the water cluster systems calculated by DFT at B3LYP/6–311++G(2d,2p) level of theory [42]. This suggests that a water cluster is similar to the hydrogen-bonded cluster in these glycolipids.

The electron affinity (*A*) is described by the LUMO energy and defined as the amount in energy released when an electron is added to the molecule to form a negative ion.[40, 43] A higher *A* of a molecule suggests that it is an electron acceptor in a charge-transfer reaction, while a molecule that has lower *A* is more likely an electron donor. Inversely, the energy of the HOMO describes the ionization potential (*IP*). A molecule having high *IP* or high *A* does not lose or accept electron easily. From the present results, **P4** has the higher *A* and **F1** the lowest one.

The electrophilicity (ω) is an index to quantify the global electrophilic nature of a molecule,[32] meaning that **P1**, which has higher ω is more electrophile than the others isomers (**P2**, **F1** and **F2**), and similar electrophilicity when compared to **P4** (Table 4). This index also measures the stabilization in energy when the system acquires an additional electronic charge; the smaller the (ω) value, the stronger the molecule stability. Hence, one can readily see from Table 4 that isomer **F1**, which is relatively the most stable, has the lowest electrophilicity followed by **P2** that has similar stability and similar electrophilicity index.

Headgroup nature

To investigate the sugar nature effect, we studied at the same level of theory the $C_{14}C_{10}$-β-*D*-xylopyranoside (**P3**) for a comparison study with its analogue $C_{14}C_{10}$-β-*D*-glucopyranoside (**P2**). Fig. 6 shows the calculated map of the MEP in the plane of the sugar ring viewed from the two sides of the sugar face (a) and (b). **P3** differs from **P2** only in the headgroup that is xylose and glucose in **P3** and **P2**, respectively. Thus, in the hydroxymethyl ($–CH_2$-OH) group on C5 carbon atom in **P2** is replaced by a proton in **P3**. The calculations showed a lower dipole moment for **P3** compared to **P2** of 3.07 and 5.18 Debye, respectively, indicating that **P2** is more polar than **P3**. This is confirmed by the molecular electrostatic potential (MEP) analysis that shows more electronegative regions (red color) for **P2** compared to **P3** (Fig.6). MEP is defined as the potential that a positively charged unit would experience at any point surrounding the molecule due to the electron density distribution. The electrostatic potential may predict

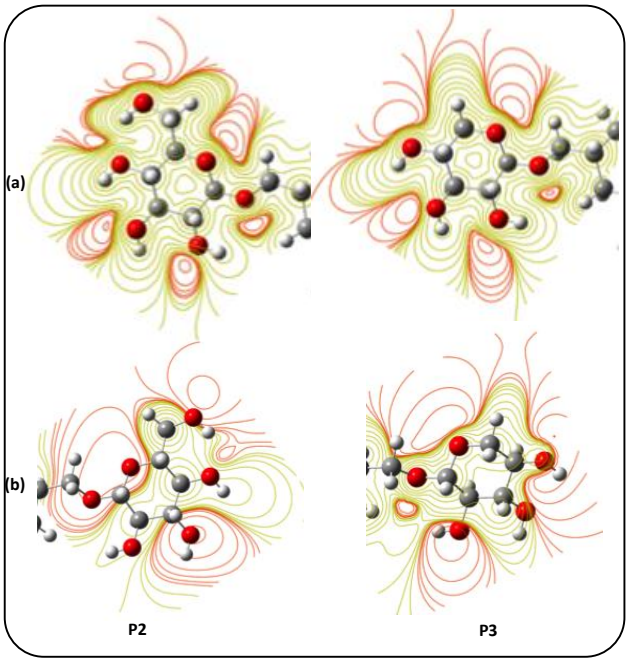

Fig. 6: Calculated MEP arrays for P2 and P3 from two views (a and b). Branched-chains were removed for clarity.

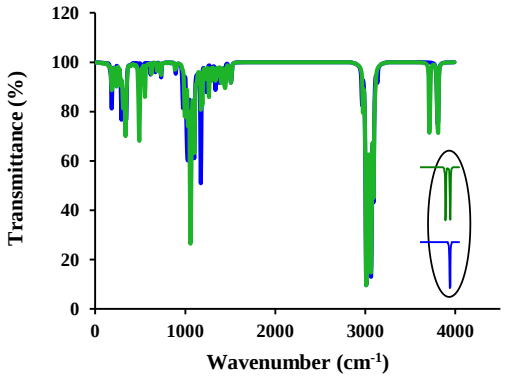

Fig. 7: Calculated IR spectra of P2 (green) and P3 (blue).

the chemical reactivity of molecules since regions of negative potential are expected to be sites of protonation and nucleophilic attack, while regions of positive potential may indicate electrophilic sites. In case of glycolipids, this analysis may explain the amphoteric nature of the sugar group. The extension of the positive electrostatic potential around the C-H group and the negative regions around the O-H group allow visualizing charge and electron density distribution within the molecule. The amphoteric nature of the sugar is clearly demonstrated and this has a direct consequences to lipidic domain heterogeneity in cell membrane, which is inherited from the chemical properties of the constituent lipids.[44], [45]

The structures of **P2** and **P3** can be clearly differentiated from the calculated IR spectra as shown in Fig. 7. This figure displayed the specific peaks around 3115 and 3715 cm^{-1} corresponding to the $–CH_2$ and –OH, respectively, forming the $–CH_2$-OH group, which characterizes **P2** and differentiates it from **P3** that is the corresponding xyloside that lacks the hydroxyl methyl group.

The MOs were also studied for **P3** and compared to those of **P2**. The HOMO and LUMO of these two molecules are not located in the same position (Fig. 5). However, their similar E_{gap} would suggest similar chemical reactivity and similar softness. The electrophilicity (ω) calculated for **P3** is slightly smaller (3.87 eV) than ω found for **P2** (3.97 eV) indicating a little lower molecular stability for **P3** compared to **P2**.

The few structural differences between **P2** (a 6-carbon sugar, a hexose) and **P3** (a 5-carbon sugar, a pentose) imply different self-assembly properties. For instance, in hydrated condition **P2** and **P3** may give rise two different liquid crystal phases, namely the reverse hexagonal phase H_{II} and the reverse discontinuous cubic phase (I_{II}) with a space group of *Fd*3*m* for **P2** and **P3**, respectively.[9, 18] The H_{II} phase is a self-assembly of long tubes arranged in a hexagonal lattice, with possible application in producing hexosome nanoparticles.[46] While *Fd*3*m* is a cubic space group consisting of a face-center cubic three-dimensional periodically ordered complex packing of two non-equivalent (in size) inverse micellar aggregates. *Fd*3*m* is usually observed for tertiary system (two lipid components) but the formation of this phase was also reported for one lipid component and water.[47], [48]

CONCLUSIONS

The current results provided new molecular insights into $C_{14}C_{10}$-*D*-glucoside isomers through quantum-based calculations, leading to a greater depth of understanding of their fundamental properties. First, through a conformational analysis, we considered the most stable conformation of each isomer that we named, **P1**, **P2**, **F1** and **F2**, corresponding to α/β pyranoside and furanoside. Similarly to their monosaccharide analogues, β-pyranoside which is energetically more stable than α-pyranoside. We also revealed that the order of stability

could be influenced by the presence of intramolecular hydrogen bonding. Such as, **F1**, the α-furanoside is the most stable isomer, which is clearly explained by the extra intramolecular hydrogen bond in **F1**. Conversely, only one intramolecular hydrogen bond can be noticed for each pyranoside, which justify the small free-energy difference (i.e., 0.68 kcal/mol) between **P1** and **P2**. **F2**, the β-furanoside, with only one intramolecular HB found to be less stable conformer because the 6-membered ring (pyranoside) defined as the more stable than the 5-membered ring (furanoside). The Boltzmann distribution of different isomers confirmed a very low value for β-furanoside. Moreover, we compared **P2**, the β-pyranoside, to its corresponding analogue with a xylose headgroup, namely $C_{14}C_{10}$-β-*D*-xylopyranoside (**P3**). Unsurprisingly, the absence of the hydroxymethyl ($-CH_2$-OH) group in the xyloside makes it less polar compared to the similar glucoside. This will directly influence their respective liquid crystal phases, which were found to be different. Indeed, in controlled conditions, **P2** and **P3** would exhibit inverted hexagonal phase (H_{II}) and cubic phase (*Fd*3*m*), respectively. From the MO study, a significant difference on their HOMO and LUMO was clearly noted. The MEP analysis also revealed different electronic properties between both systems. Yet, both of these molecules exhibit inverse cubic phases, which suggest probably the presence of two different hydrogen-bond clusters, one for each layer, relating to the microscopic heterogeneity nature of lipid self-assembly. This may also explain important phenomena in membrane physics called lipid asymmetry and lipid microdomain, which are resulting from the irregularity of lipid distribution between the two leaflets or within the same leaflet, respectively. Although the current results allow understanding the electro-molecular features for single glycolipids, rationalizing intermolecular interactions such as intermolecular hydrogen bonding is essential towards establishing a full understanding of glycolipids self- assemblies. Results for such studies can be conducted by a subsequent Molecular Dynamic (DM) analysis.

Acknowledgments

The authors gratefully thank the High Impact Research Grant UM.C/625/1/HIR/MOHE/05 (Malaysia), King Faisal University (KSA) and the Center for Information Technology (PTM) for financial support and computing facilities. IB is grateful to Prof. Dr. Jean-Frédéric F. Weber from Universiti Teknologi MARA (UiTM), Puncak Alam, Malaysia, for fruitful discussions.

Received : Aug. 31, 2018 ; Accepted :Jan. 28, 2019

REFERENCES

[1] Bahadur B., "Liquid Crystals - Applications and Uses": (Volume 1), World Sci, (1990).

[2] Cox T.M., Future Perspectives for Glycolipid Research in Medicine., *Philos Trans R Soc Lond B Biol Sci*, **358**(1433): 967–973 (2003).

[3] Faivre V., Rosilio V., Interest of Glycolipids in Drug Delivery: from Physicochemical Properties to Drug Targeting, *Expert Opin Drug Deliv*, **7**(9): 1031–1048 (2010).

[4] Inès M., Dhouha G., Glycolipid Biosurfactants: Potential Related Biomedical and Biotechnological Applications, *Carbohydr. Res.*, **416**: 59–69 (2015).

[5] Kitamoto D., Isoda H., Nakahara T., Functions and Potential Applications of Glycolipid Biosurfactants--from Energy-Saving Materials to Gene Delivery Carriers, *J. Biosci. Bioeng.*, **94**(3): 187–201 (2002).

[6] Lourith N., Kanlayavattanakul M., Natural Surfactants Used in Cosmetics: Glycolipids, *Int. J. Cosmet. Sci.*, **31**(4): 255–261 (2009).

[7] Vill V., Hashim R., Carbohydrate Liquid Crystals: Structure–Property Relationship of Thermotropic and Lyotropic Glycolipids," *Curr. Opin. Colloid. Interface. Sci.*, **7**(5): 395–409 (2002).

[8] Garidel P., Kaconis Y., Heinbockel L., Wulf M., Gerber S., Munk A., Vill V., Brandenburg K., Self-Organisation, Thermotropic and Lyotropic Properties of Glycolipids Related to their Biological Implications, *Open Biochem J*, **9**: 49–72 (2015).

[9] Liew C.Y., Salim M., Zahid N.I., Hashim R., Biomass Derived Xylose Guerbet Surfactants: Thermotropic and Lyotropic Properties from Small-Angle X-Ray Scattering, *RSC Advances: An International Journal to Further the Chemical Sciences*, **5**(120): 99125–99132 (2015).

[10] Manickam Achari V., Nguan H. S., Heidelberg T., Bryce R. A., Hashim R., Molecular Dynamics Study of Anhydrous Lamellar Structures of Synthetic Glycolipids: Effects of Chain Branching and Disaccharide Headgroup, *J. Phys. Chem. B*, **116**(38): 11626–11634 (2012).

[11] Zahid N. I., Conn C.E., Brooks N.J., Ahmad N., Seddon J.M., Hashim R., Investigation of the Effect of Sugar Stereochemistry on Biologically Relevant Lyotropic Phases from Branched-Chain Synthetic Glycolipids by Small-Angle X-Ray Scattering, *Langmuir*, **29**(51): 15794–15804 (2013).

[12] Bayach I., Achari V.M., Iskandar W.F.N.W., Sugimura A., Hashim R., Computational Insights Into octyl-D-xyloside Isomers Towards Understanding the Liquid Crystalline Structure: Physico-Chemical Features, *Liq. Crys.*, **43**(10): 1503–1513 (2016).

[13] Kotena Z.M., Behjatmanesh–Ardakani R., Hashim R., AIM and NBO Analyses on Hydrogen Bonds Formation in Sugar-Based Surfactants (α/β-d-Mannose and n-octyl-α/β-d-mannopyranoside): A Density Functional Theory Study, *Liq. Crys.*, **41**(6): 784–792 (2014).

[14] Mosapour Kotena Z., Behjatmanesh-Ardakani R., Hashim R., Manickam Achari V., Hydrogen Bonds in Galactopyranoside and Glucopyranoside: A Density Functional Theory Study, *J. Mol. Model*, **19**(2): 589–599 (2013).

[15] O'Lenick A.J., Guerbet Chemistry, *J. Surfactants Deterg.*, **4**(3): 311–315 (2001).

[16] Minamikawa H., Hato M., Reverse Micellar Cubic Phase in a Phytanyl-Chained Glucolipid/Water System, *Langmuir*, **14**(16): 4503–4509 (1998).

[17] Barauskas J., Cervin C., Tiberg F., Johnsson M., Structure of Lyotropic Self-Assembled Lipid Nonlamellar Liquid Crystals and Their Nanoparticles in Mixtures of Phosphatidyl Choline and Alpha-Tocopherol (Vitamin E)," *Phys. Chem. Chem. Phys.*, **10**(43): 6483–6485 (2008).

[18] Brooks N.J., Hamid H.A.A., Hashim R., Heidelberg T., Seddon J.M., Conn Ch.E., Mirzadeh Husseini S.M., Ldayu Zahid N., Duali Hussen R.S., Thermotropic and Lyotropic Liquid Crystalline Phases of Guerbet Branched-Chain -D-Glucosides, *Liq. Crys.*, **38**(11–12): 1725–1734 (2011).

[19] Lee C., Yang W., Parr R.G., Development of the Colle-Salvetti Correlation-Energy Formula into a Functional of the Electron Density, *Phys. Rev. B*, **37**(2): 785–789 (1988).

[20] Becke A. D., Density-Functional Thermochemistry. III. The Role of Exact Exchange, *J. Chem. Phys.*, **98**: 5648–5652 (1993).

[21] Biegler-König F., Schönbohm J., Update of the AIM2000-Program for Atoms in Molecules, *J. Comput. Chem.*, **23**(15): 1489–1494 (2002).

[22] Reed A.E., Curtiss L.A., Weinhold F., Intermolecular Interactions from a Natural Bond Orbital, Donor-Acceptor Viewpoint, *Chem. Rev.*, **88**: 899-926 (1988).

[23] Runge E., Gross E.K.U., Density-Functional Theory for Time-Dependent Systems, *Phys. Rev. Lett.*, **52**(12): 997–1000 (1984).

[24] Cossi M., Barone V., Cammi R., Tomasi J., Ab initio Study of Solvated Molecules: A New Implementation of the Polarizable Continuum Model, *Chem Phys Lett*, **255**(4): 327–335 (1996).

[25] Frisch M.J. *et al.*, "Gaussian 09," Gaussian, Inc., Wallingford CT, (2009).

[26] Dennington R., Keith T., Millam J., "GaussView," Semichem Inc, (2009).

[27] Humphrey W., Dalke A., Schulten K., VMD: Visual Molecular Fynamics, *J Mol Graph*, **14**(1): 33-38 (1996).

[28] Angyal S.J., The Composition and Conformation of Sugars in Solution, *Angew Makromol. Chem. Edition in English*, **8**(3): 157-166 (1969).

[29] Hashim R., Hashim H.H.A., Rodzi N.Z.M., Hussen R.S.D., Heidelberg T., Branched Chain Glycosides: Enhanced Diversity for Phase Behavior of Easily Accessible Synthetic Glycolipids, *Thin Solid Films*, **509**(1): 27–35 (2006).

[30] Los J.M., Simpson L.B., Wiesner K., The Kinetics of Mutarotation of D-Glucose with Consideration of an Intermediate Free-aldehyde Form, *J. Am. Chem. Soc.*, **78**(8): 1564–1568 (1956).

[31] Bader R.F.W., Essén H., The Characterization of Atomic Interactions, *Journal of Chemical Physics*, **80**: 1943–1960 (1984).

[32] Chattaraj P.K., Sarkar U., Roy D.R., Electrophilicity Index, *Chem. Rev.*, **106**(6): 2065–2091 (2006).

[34] Gatti C., Macchi P., "Modern Charge-Density Analysis", Springer Science & Business Media, (2012).

[33] Hobza P., 2 Theoretical Studies of Hydrogen Bonding, *Annu. Rep. Prog. Chem., Sect. C: Phys. Chem.*, **100**: 3–27 (2004).

[35] Lee S.L., Debenedetti P.G., Errington J.R., A Computational Study of Hydration, Solution Structure, and Dynamics in Dilute Carbohydrate Solutions, *J. Chem. Phys.*, **122**(20): 204511 (2005).

[36] Zhao L., Ma K., Yang Z., Changes of Water Hydrogen Bond Network with Different Externalities, *Int. J. Mol. Sci.*, **16**(4): 8454–8489 (2015).

[37] Misran O., Timimi B.A., Heidelberg T., Sugimura A., Hashim R., Deuterium NMR Investigation of the Lyotropic Phases of Alkyl β-glycoside/D2O Systems, *J. Phys. Chem. B.*, **117**(24): 7335–7344 (2013).

[38] Manickam Achari V., Bryce R.A., Hashim R., Conformational Dynamics of Dry Lamellar Crystals of Sugar Based Lipids: an Atomistic Simulation Study, *PLOS ONE*, **9**(6): e101110 (2014).

[39]Mizuseki H., Belosludov R.V., Farajian A.A., Lgarashi N., Wang J.T., Chen H., Majumder Ch., Miura Sh., Kawazoe Y., Molecular Orbital Analysis of Frontier Orbitals for Molecular Electronics: a Case Study of Unimolecular Rectifier and Photovoltaic Cell, *Sci. Technol. Adv. Mater.*, **4**(4): 377-382 (2003).

[40] Bader R.F.W., "An Introduction to the Electronic Structure of Atoms and Molecules", 1st ed., Toronto: Clarke, Irwin, (1970).

[41] Pearson R.G., The Electronic Chemical Potential And Chemical Hardness, *J. Mol. Struct: Theochem*, **255**: 261–270 (1992).

[42] Rai D., Kulkarni A.D., Gejji S.P., Bartolotti L.J., Pathak R.K., Exploring Electric Field Induced Structural Evolution of Water Clusters, $(H_2O)N$ [N = 9–20]: Density Functional Approach, *J. Chem. Phys.*, **138**(4): 044304 (2013).

[43] Bader R.F.W., "Atoms in Molecules: A Quantum Theory", Oxford, New York: Oxford University Press, (1994).

[44] Abou-Zied O.K., Zahid N.I., Khyasudeen M.F., Giera D.S., Thimm J.C., Hashim R., Detecting Local Heterogeneity and Ionization Ability In The Head Group Region of Different Lipidic Phases Using Modified Fluorescent Probes, *Scientific Reports*, **5**: 8699 (2015).

[45] Ishitsuka R., Yamaji-Hasegawa A., Makino A., Hirabayashi Y., Kobayashi T., A Lipid-Specific Toxin Reveals Heterogeneity of Sphingomyelin-Containing Membranes, *Biophys. J.*, **86**(1): 296–307 (2004).

[46] Amar-Yuli I., Wachtel E., Shoshan E.B., Danino D., Aserin A., Garti N., Hexosome and Hexagonal Phases Mediated by Hydration and Polymeric Stabilizer, *Langmuir*, **23**(7): 3637–3645 (2007).